Application of orientation mapping in TEM and SEM for study of microstructural evolution during annealing. Example: Aluminum alloy with bimodal particle distribution.

Krzysztof Sztwiertnia

Institute of Metallurgy and Materials Science PAS, 25 Reymonta St., 30-059 Krakow, Poland

The characterization of microstructures has advanced in great part to the development of new generations of computer-controlled electron microscopes. New technologies have improved spatial resolution and have increased the rate of collecting and processing of large quantities of data. The Orientation Imaging Microscopy (OIM) is a well-established technique for studying and quantifying microstructures and can determine crystallographic orientations and topography by using Electron Back Scattered Diffraction (EBSD) in a Scanning Electron Microscope (SEM) e.g. [1]. The main concept behind this technique is the automatic collection and indexing of many diffraction patterns that are correlated with sample coordinates. Characteristics based on the sets of measured orientations provide essential information about the grains, grain boundaries and about local crystallographic lattice deformation. Systems created using EBSD in SEM are very common, and that one's commercially available are essentially fully automated e.g. [1, 2].

Nevertheless, the spatial resolution of SEM measurements is strongly dependent on the type of electron gun and material being investigated. The best achievable spatial resolution in special cases is in the order of about 30 nm, however practical limits are about 100 nm. This limitation restricts the application of SEM in investigating very fine-grained and deformed materials. In order to obtain better spatial and angular resolution, similar systems were developed for a Transmission Electron Microscope (TEM) [2, 3, 4]. Despite some restrictions, such as the unsolved problems with image analysis, difficulties in the measurement automation and sample preparation, the OIM technique in TEM offers spatial resolution better than 10 nm and can be used for quantitative analysis of the microstructure at the nanoscale. Such a system, built in the Institute of Metallurgy and Materials Science [4, 5, 6], was used for study of of recrystallization in 6013 aluminum alloy. This alloy was chosen here as a prototype material that represents a group of commercial alloys with a bimodal second phase particle distribution. The second-phase particles are used to control the strengthening, grain size as well as the texture of alloy. Such alloys can be interesting for considering the role of second phase particles in a recrystallization process e.g. [7, 8, 9, 10]. There is a need for investigating the early stages of the recrystallization, based on the analyzing changing orientation topography during annealing [11 - 13].

Material for testing was supersaturated, then aged. In this way the relatively uniform distribution of stable particles, both small ($<<1\mu m$) and large ($>1\mu m$) ones, were obtained. The aged samples were reversible cold-rolled and then annealed in a calorimeter to achieve defined stages of recrystallization. During cold rolling, the laminar structure and deformation

zones (DZ) around large particles (both with characteristic local textures) are formed e.g. [9-12]. The microstructure of the DZs was built of small grains (50-200 nm) and distorted

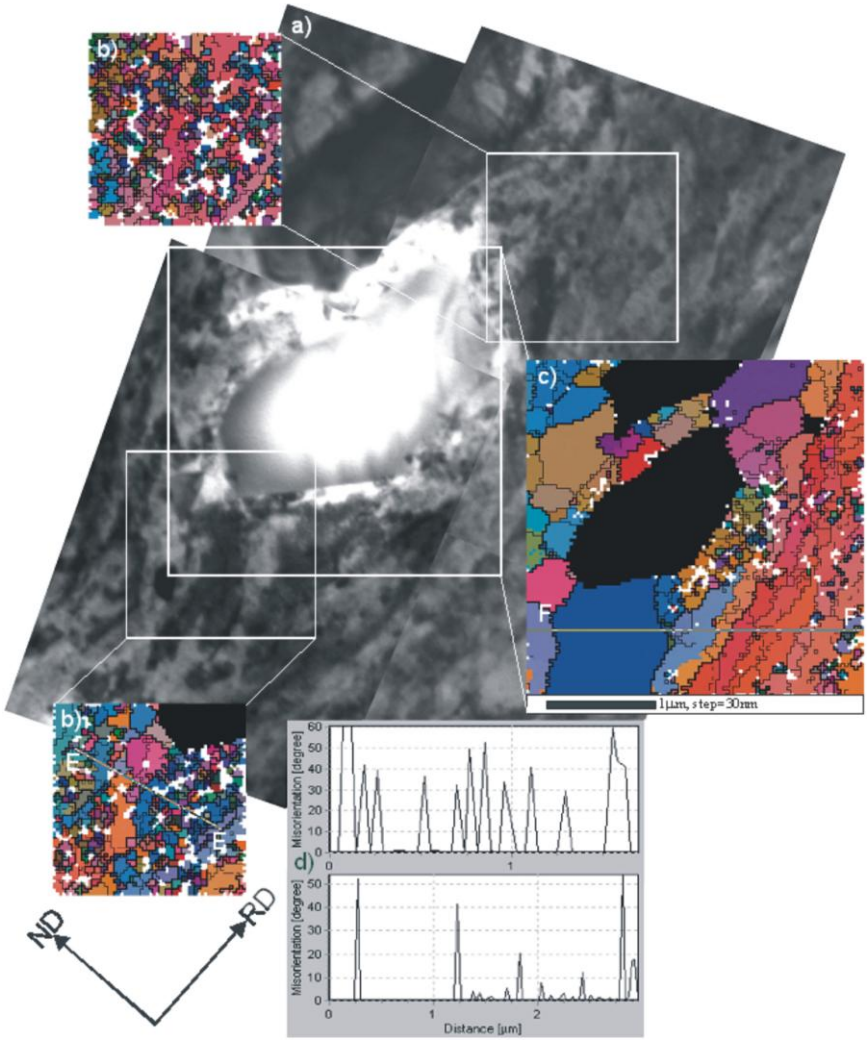

Fig. 1. a) As-deformed microstucture of 75% cold-rolled 6013 alloy, the deformation zone around the large particle, longitudinal section, TEM. Orientation topographies in areas of the deformation zone before (b) and after (c) heating *in situ* in TEM; particles of the second phase – black, white regions – not indexed; thick lines – high angles grain boundaries, thin lines – low angles grain boundaries. d) Examples of disorientation angle profiles along E-E and F-F, respectively.

fragments of microbands, Fig. 1 a, b. The strong orientation changes, more than 15^0, identify high angle grain boundaries (HAGB) lying on distances lower than 200 nm, Fig. 1d. *In situ* investigations in TEM[1] as well as calorimetric measurements, combined with orientation mapping in TEM and SEM, demonstrate, that recrystallization can be considered as a number of partly overlapping processes, proceeding in two stages, Fig. 2, 3, 4. These stages correspond to the two separated peaks of the stored energy release, Fig. 2. In the initial stage,

[1] Already in the first *in-situ* observations in TEM performed by Bailey [15] and Hu [16], it was noted that there are some differences that can occur between the recrystallization process taking place in a fine foil and the one occurring in a massive sample. As a consequence of those concerns, many scientists have been sceptical as regards the *in-situ* tests in TEM. However, we should remember that other experiments, such as [17-19], make it possible to select the experiment conditions in such a way so as to keep the changes, observed during the annealing of fine foils, at least close to those taking place in a massive sample. In our work, the *in-situ* tests were verified on the basis of the combined calorimetric-microscopic measurements.

the DZs act as sites for particle stimulated nucleation (PSN) e.g. [7-9]. There occurs also the growth of the nuclei. However, the migration of HAGBs was limited to the areas of DZs only, Fig. 1 c, 3.

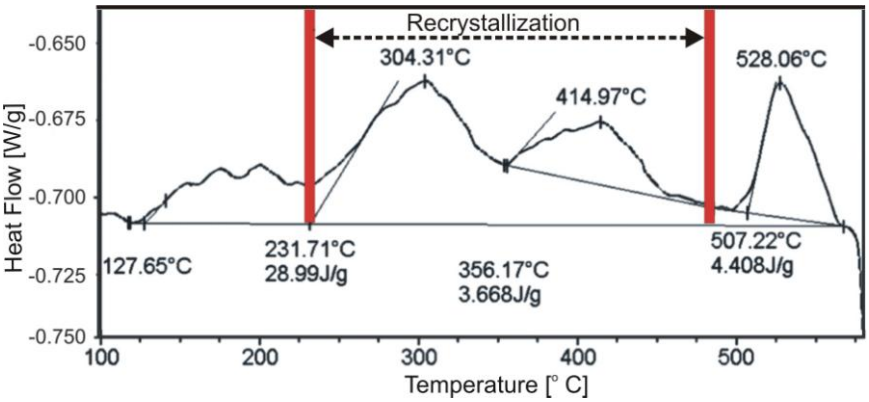

Fig. 2. Example of the heat flow, representing release of stored energy from cold-rolled 6013 aluminum alloy, the differential calorimeter.

In regions of matrix, outside the DZs, a certain enlargement of new grains in the sheet plane was also observed, Fig. 4 a, b. The formation of grains elongated primarily in the direction parallel to rolling direction (RD) may be correlated to the processes of local recovery [13], triggered in the DZs, that continued to develop along the bands of the deformed matrix in the directions of low orientation gradients. The elongated grains appear due to the annihilation of low angle grain boundaries (LAGB) between chains of subgrains lying in layers parallel to the sheet plane, Fig. 3. As a consequence, new grains often have a plate-like habit, with the shorter axis parallel to the sheet plane normal direction (ND). Their lengths, along RD may exceed 50 μm, whilst their thickness corresponded approximately to the distances between HAGBs in ND outside DZs and did not exceed 1-2 μm, Fig 2 b.

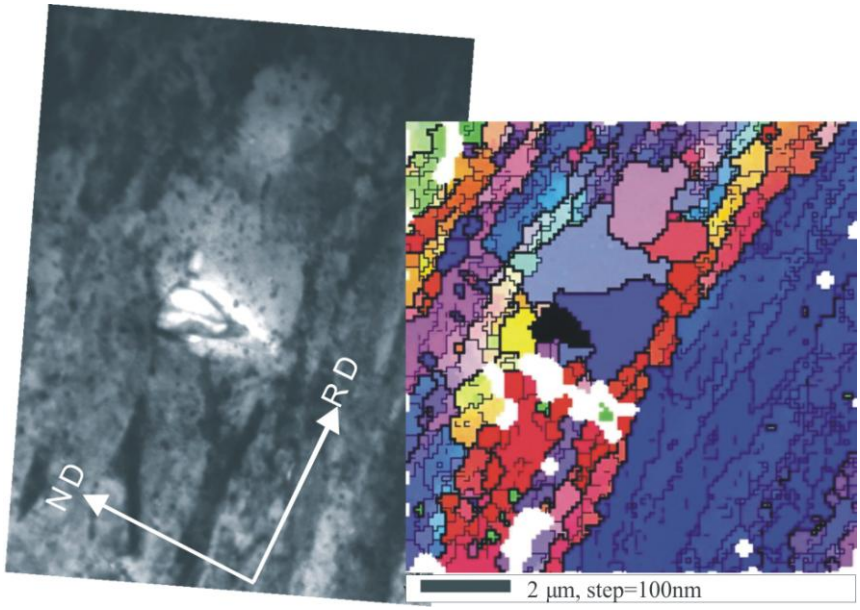

Fig. 3. Microstructure of the 6013 aluminum alloy after 75 % cold rolling and then heating in a calorimeter to 330 ^{o}C, DZ around the black-marked precipitate particle, thick lines – HAGBs, thin lines – LAGBs, longitudinal section, TEM.

In the second stage, HAGBs were observed to migrate in the direction of high orientation gradient. This migration, mostly in the ND, was limited to "free areas" of the deformed matrix between bands of the new grains formed in the DZs in the initial stage of recrystallization, Fig. 4 c.

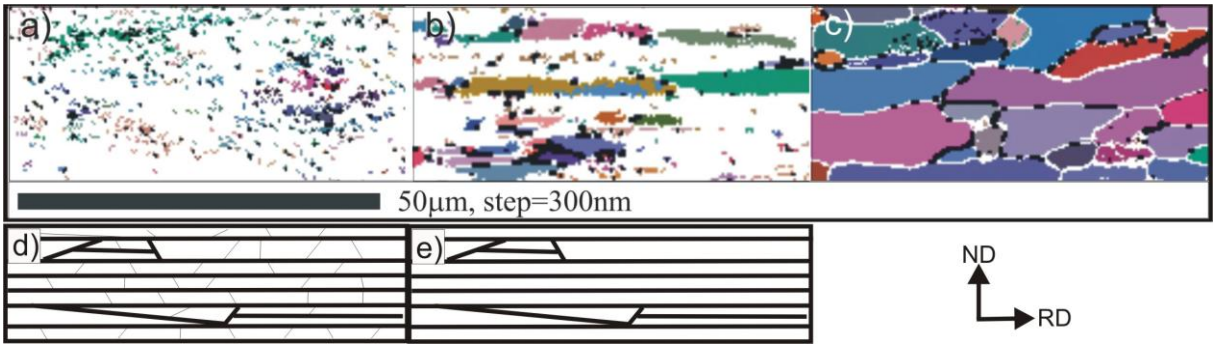

Fig. 4. 6013 aluminum alloy, 75% cold rolled and subsequently heated in the calorimeter to: (a) 330 ^{o}C, (b) 350 ^{o}C and (c) 480 ^{o}C; orientation topographies in areas of the new grains, SEM; regions of unsolved diffractions (approximately corresponding to the deformed areas) – white, EBSD/SEM/FEG. d) and e) Schematic presentation of the deformed microstructure of the matrix before and after annealing to the temperatures from the end of the first recrystallization peak, Fig. 2; thin lines – LAGBs, thick lines – HAGBs.

References

1. S.I. Wright, B.L. Adams, Met. Trans. A 23 (1992) 759.
2. S. Zaefferer, J. Appl. Cryst. 33 (2000) 10.
3. R.A. Schwarzer, Ultramicroscopy 67 (1997) 19.
4. J.J. Fundenberger, A. Morawiec, E. Bouzy, J.S. Lecomte, Ultramicroscopy 96 (2003) 127.
5. A. Morawiec, J. Appl. Cryst. 32 (1999) 788.
6. A. Morawiec, J.J. Fundenberger, E. Bouzy, & J.S. Lecomte, Appl. Cryst. 35 (2002) 287.
7. F. J. Humphreys, Metal Sci.13 (1979) 136.
8. F.J. Humphreys, F.J. and M. Hatherly, Recrystallization and Related Annealing Phenomena, Pergamon Press, Oxford, 2002.
9. M.G. Ardakani, F.J. Humphreys, Acta metall. mater. 42 (1994) 763.
10. E. Nes, Acta Metall. 24 (1976) 391.
11. K. Sztwiertnia, J. Morgiel, E. Bouzy, Arch. Metall. Mater. 50 (2005) 119.
12. M. Bieda, K. Sztwiertnia, A. Korneva, T. Czeppe, R. Orlicki, Sol. St. Phen., 16 (2010) 13.
13. K. Sztwiertnia, M. Bieda, A. Korneva, G. Sawina, Inz. Mater. 157-158 (2007) 476.
14. R.D, Doherty and J. Szpunar. Acta Metall. (1984) 32, 1789.
15. Bailey J.E.: Phil. Mag., **5 (**1960) 833.
16. Hu H.: Electron Microscopy and Strength of Crystals, Interscience, London, 1963, p. 564.
17. Roberts W., Lehtinen B.: Phil. Mag., **26 (**1972) 1153.
18. Hutchinson W.B., Ray R.K.: Phil. Mag., **28 (**1973) 953.
19. Sztwiertnia K., Haessner F.: Mater. Sci. Forum, **157-162 (**1994) 1069.